



Memory versus effector immune responses in oncolytic virotherapies



Cicely Macnamara, Raluca Eftimie*

Division of Mathematics, University of Dundee, Dundee DD1 4HN, United Kingdom

AUTHOR - HIGHLIGHTS

- We model memory and effector immune responses on tumour–virus interactions.
- The model shows that cancer control is associated with high numbers of effector cells.
- Effector cell persistence requires high initial memory cell population.
- Cancer control from dormant state cannot be predicted by the initial memory size.

ARTICLE INFO

Article history:

Received 26 August 2014

Received in revised form

27 March 2015

Accepted 1 April 2015

Available online 13 April 2015

Keywords:

Cancer modelling

Effector and memory cells

Tumour control

Tumour dormancy

ABSTRACT

The main priority when designing cancer immuno-therapies has been to seek viable biological mechanisms that lead to permanent cancer eradication or cancer control. Understanding the delicate balance between the role of effector and memory cells on eliminating cancer cells remains an elusive problem in immunology. Here we make an initial investigation into this problem with the help of a mathematical model for oncolytic virotherapy; although the model can in fact be made general enough to be applied also to other immunological problems. According to this model, we find that long-term cancer control is associated with a large number of persistent effector cells (irrespective of the initial peak in effector cell numbers). However, this large number of persistent effector cells is sustained by a relatively large number of memory cells. Moreover, the results of the mathematical model suggest that cancer control from a dormant state cannot be predicted by the size of the memory population.

© 2015 Elsevier Ltd. All rights reserved.

1. Introduction

It is well known that after successful reaction to a pathogen, long-lasting immunity can be stimulated (Kumar et al., 2011). Harnessing this natural defence system, through the use of vaccines, has long been important in the fight against infections and diseases (Bachmann and Jennings, 2010; Dermime et al., 2002). More recently immune mechanisms have been employed to combat cancer through various immunotherapies such as virotherapies, adoptive transfer of immune cells, cytokine therapies or antibody therapies. The low success rates of these immunotherapies are mainly caused by the fact that the immune–cancer interactions are still not fully understood.

One of the emerging cancer therapies is oncolytic virotherapy, which involves both the direct action of tumour cell destruction by a virus (that usually carries tumour-associated antigens (TAAs)

and the indirect action of anti-tumour immunity (as the immune cells learn, through interaction with the virus, to recognise the TAAs) (Kelly and Russell, 2007; Pol et al., 2012; Russell et al., 2012). The interactions between the immune cells and the viruses lead to short term (or therapeutic) and long term (or prophylactic) immunity, which can be naively characterised by effector and memory immune cells, respectively (Bachmann and Jennings, 2010). In the short term effector cells act to eliminate a pathogen, while in the long-term memory cells act to prevent its reoccurrence. Memory cells are antigen-specific; they are stored after a pathogen has been eliminated (Crotty and Ahmed, 2004; Klebanoff et al., 2006; Wodarz, 2006) and are capable of generating new effector cells (Sallusto et al., 2004). Successful cancer treatment protocols seek persistent protection against the tumour whether through permanent elimination or control.

An important research question in immunology, still unanswered at this moment, refers to whether it is effector or memory cells which play the most important role in successful treatment protocols. It has been posited that multiple treatment protocols are likely to provide better success in immune therapies. In particular, for cancer therapies, multiple and subsequent treatments provide the

* Corresponding author. Tel.: +44 1382 384488; fax: +44 1382 385516.

E-mail addresses: c.k.macnamara@dundee.ac.uk (C. Macnamara), reftimie@maths.dundee.ac.uk (R. Eftimie).

possibility of activating the memory cells, which can then be used to generate a stronger more targeted response against the tumour (Klebanoff et al., 2005; van Duikeran et al., 2012; Wherry and Ahmed, 2004; Zhang, 2007). On the other hand, there is increasing evidence that long-term cancer control is accompanied by high numbers of effector cells (Baitsch et al., 2011; Berezhnoy et al., 2014; Paulis et al., 2013). Understanding the delicate balance between the anti-tumour role of effector and memory cells will improve the existent anti-cancer treatments.

Mathematical models (see, for example, Bozic et al., 2012; Eftimie et al., 2011b; Ferreira et al., 2005; Karez et al., 2006; Komarova and Wodarz, 2010; Paiva et al., 2009, 2011; Rommelfanger et al., 2012; Wein et al., 2003; Wodarz et al., 2012; Wodarz and Komarova, 2009 and the references therein) have shown that possible outcomes for anti-tumour therapies are as follows: tumour elimination, tumour dormancy, tumour escape or tumour control. A distinction between dormancy and control can be made: tumour control occurs when the tumour is held permanently at a constant but relatively low size, while tumour dormancy is described as a prolonged period in which the tumour remains small and as such is both asymptomatic and undetectable but will at some stage grow again (Quesnel, 2008). Although the nature of the biological mechanisms leading to tumour dormancy is not fully known (Almog, 2010; Uhr and Pantel, 2011), one possible means is through tumour-immune interactions, the so called immune-mediated dormancy (Farrar et al., 1999; Teng et al., 2008; Wilkie and Hahnfeldt, 2013a). It is thought that a constant interplay between the tumour and immune cells can lead to this temporary equilibrium, but eventually one population will overpower the other and either the tumour will “escape” and grow rapidly or it will be eliminated (Teng et al., 2008; Wilkie and Hahnfeldt, 2013b). Clearly, from a clinical outlook tumour escape is a negative outcome and cancer elimination is the goal of any treatment protocol. However, as we will discuss here (and as suggested before Gatenby, 2009), tumour control may be the only possible approach when tumour elimination is impossible. Tumour dormancy, although of short term therapeutic benefit, presents a clinical challenge in the long-term as predictions regarding its end stage (escape or elimination) may be unlikely.

In this paper, we will introduce and investigate a mathematical model for oncolytic virotherapy, which allows us to study the balance between the memory and effector immune responses that can control tumour growth or lead to tumour dormancy. Although there are many mathematical models for cancer virotherapies (see, for example, Bajzer et al., 2008; Biesecker et al., 2010; Friedman et al., 2006; Komarova and Wodarz, 2010; Wein et al., 2003; Wodarz, 2001; Wu et al., 2004 and the references therein), the model investigated in this study is based on a more complex ODE model described in Eftimie et al. (2011b), which incorporated effector and memory immune responses and replicated a treatment protocol derived in Bridle et al. (2010). In that protocol, two viruses that carried the same tumour-associated antigen (human dopachrome tautomerase, or hDCT) were administered 14 days apart. The first virus, Adenovirus (Ad), acted as a vaccine virus by provoking an immune response against the tumour antigens. As this immune response receded, memory cells were created. The second virus, Vesicular Stomatitis Virus (VSV), was an oncolytic virus. This virus not only destroyed the cancer cells directly, but provoked a much stronger immune response to the tumour antigens due to the memory cells created in the first phase. The protocol, tested on mice, did not eradicate tumours in the majority of cases but did lead to improved survival times (compared with survival times for mice treated with just one virus). The mathematical model introduced in this study focuses on the second part of this treatment protocol, i.e., on the oncolytic virus (injected after the formation of memory cells). Using this model, we will investigate how differences in the magnitude of the initial

memory cell population lead to control, dormancy or escape of tumour cells. We will also determine the role of parameters governing the behaviour of effector cells on the outcome of the treatment.

The paper is structured as follows. In Section 2 we describe the mathematical model. In Section 3 we begin our investigation of the long-term dynamics of this model by focusing on the steady states and their stability. To get a better understanding of the balance between effector and memory immune responses, in Section 4 we discuss the steady-state behaviour of a simplified virus-free model. In fact, this simplified model is general enough to be applied to any immunotherapy and so may permit us to make stronger conclusions about the relative importance of different immune cell types in targeting cancer. In Section 5 we investigate numerically the long-term dynamics of both the full model and the simplified model paying particular attention to the effects of varying the initial memory cell population size. Finally, in Section 6 we return to the simplified model and investigate the parameters that govern the effector cells. We conclude in Section 7 with a summary and discussion of the results.

2. Model description

To model the tumour-immune-virus interactions, we focus on the following populations: the uninfected (x_u) and infected (x_i) tumour cells, the memory (x_m) and effector (x_e) immune cells, and the virus particles (x_v). We assume that the virus particles are VSV particles, and that the effector/memory cells are CD8⁺ T cells. The equations below, which are adapted from Eftimie et al. (2011b), take into account the fact that effector cell proliferation is stimulated by both the presence of the free virus particles (as considered in Eftimie et al., 2011b) and the uninfected tumour cells (an aspect not considered in Eftimie et al., 2011b). Since the data in Bridle et al. (2010) ignored the spatial aspect of solid tumours, we decided to use an ODE model, with saturated interaction terms accounting for some of the tumour spatial structure:

$$\frac{dx_u}{dt} = rx_u \left(1 - \frac{x_u + x_i}{k}\right) - d_v \frac{x_u}{h_u + x_u} x_v - d_u x_u \frac{x_e}{h_e + x_e}, \quad (1a)$$

$$\frac{dx_i}{dt} = d_v \frac{x_u}{h_u + x_u} x_v - \delta x_i - d_u x_i \frac{x_e}{h_e + x_e}, \quad (1b)$$

$$\frac{dx_m}{dt} = p_m \frac{x_v}{h_v + x_v} x_m \left(1 - \frac{x_m}{M}\right), \quad (1c)$$

$$\frac{dx_e}{dt} = p_e \frac{x_v + x_u}{h_v + x_v + x_u} x_m - d_e x_e - d_t x_u x_e, \quad (1d)$$

$$\frac{dx_v}{dt} = \delta b x_i - \omega x_v. \quad (1e)$$

These equations incorporate the following biological assumptions:

- The uninfected tumour cells grow logistically at a rate r , up to their carrying capacity k . We use logistic growth because some experimental studies show evidence of a reduced rate of tumour growth at larger sizes (see, for example, the *in vivo* and *in vitro* growth of various human and rodent solid tumours shown in Guiot et al., 2003; Laird, 1964; Looney et al., 1980). An alternative would be to assume straight exponential growth (or other growth laws Bonate, 2011), which might lead to different results but are not investigated here. The large carrying capacity k (see Table A2 for its value) – chosen to correspond to the humane endpoint for experimental protocols with mice (Bridle et al., 2010; N.I.H., O.A.C.U., 1996) – allows us to

investigate the role of oncolytic therapy on large tumours (Ikeda et al., 1999). The uninfected tumour cells are infected by the virus particles at a rate d_v , and are killed by the effector cells at a rate d_u . The saturated form of the tumour–virus interaction term accounts in part for the spatial structure of the tumour, which leads to reduced interactions between the tumour cells and viruses (studies showing that viruses usually infect only a small number of tumour cells Breitbach et al., 2007). Finally, the saturated form of the tumour–immune interaction term accounts for the reduced number of activated immune cells that reach and interact with the tumour cells (Gajewski et al., 2013).

- The infected tumour cells die at a rate δ (when they burst to let the replicated virus particles out). Also, they are killed by the effector cells at a rate d_u .
- The memory cells proliferate, at a rate p_m , in the presence of virus particles (virus antigens). These cells have a carrying capacity M , which models the competition for space between memory cells or competition for antigens (Antia et al., 1998). We assume here that the memory cells persist for a very long time (compared to the effector and tumour cells), and thus we ignore their natural death rate. Parameter h_v denotes the half-concentration of viral antigens that trigger the memory response. The saturated form of the virus-induced memory response accounts for the limited proliferation of memory cells in response to virus particles.
- The effector cells are the result of de-differentiation of memory cells in the presence of antigens (both virus antigens and tumour antigens). The de-differentiation rate is p_e . These effector cells have a natural death rate of d_e , and can be inactivated by the tumour cells at a rate d_t . For simplicity, we decided to use the same half-concentration h_v for the antigens (both viral and tumour antigens). However, as we will discuss in Section 6, the magnitude of this parameter does not have a great influence on the dynamics.
- The virus particles are produced by the infected tumour cells at a rate δb , where δ is the death rate of infected cells and b is the burst size (i.e., the number of particles inside an infected cell). Finally, these particles are eliminated by the body at a rate ω .

For a more detailed description of the model, see Eftimie et al. (2011b). Note that the 2-compartment model in Eftimie et al. (2011b) accounted for the delay in the effector immune response following virus stimulation. To gain a better understanding of the

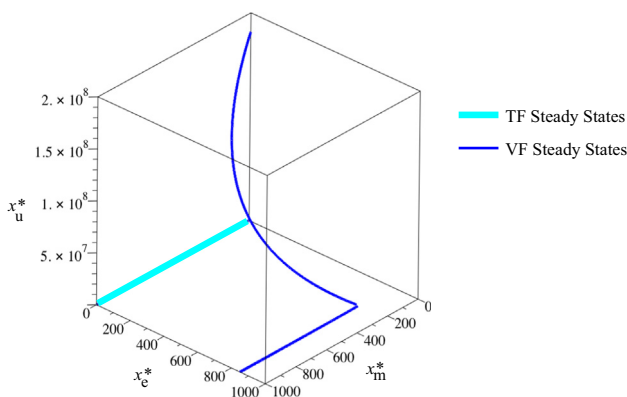


Fig. 1. A plot showing the possible virus-free steady states of system (1). The tumour-free (TF) states are given by the cyan thick line, the tumour-present virus-free (VF) states are given by the dark blue curve. (For interpretation of the references to color in this figure caption, the reader is referred to the web version of this article.)

key parameters in tumour–immune–virus dynamics, in this paper we decided to ignore such a delay.

We emphasise that many of the biological processes considered in this mathematical model could have been formulated differently (see the models in Bajzer et al., 2008; Biesecker et al., 2010; Eftimie et al., 2011a,b; Friedman et al., 2006; Komarova and Wodarz, 2010; Wein et al., 2003; Wodarz, 2001; Wu et al., 2004). For example, the proliferation of memory cells following virus stimulation was implemented differently in a previous study (Eftimie et al., 2011b), which considered a different pathway for memory differentiation – one of the multiple pathways suggested in the literature (Kaech et al., 2002). Equally, the tumour–immune and tumour–virus interactions could have been modelled using bilinear terms, rather than the saturated forms we give, and the tumour growth could have been modelled using a Gompertzian or exponential form (Benzekry et al., 2014; Komarova and Wodarz, 2010; Marusić and Vuk-Pavlovic, 1993). However, it is not the goal of this paper to investigate the impact of the different possible descriptions of interaction terms on the outcomes of the model. Rather, it is to choose an example of interaction terms and use them to take a first look at the potential importance of effector versus memory cells during viral therapies.

3. Steady states and stability

We start the investigation of model (1) by studying first its long-term dynamics. To this end, we identify all possible steady states and determine their stability. The parameter values investigated in this

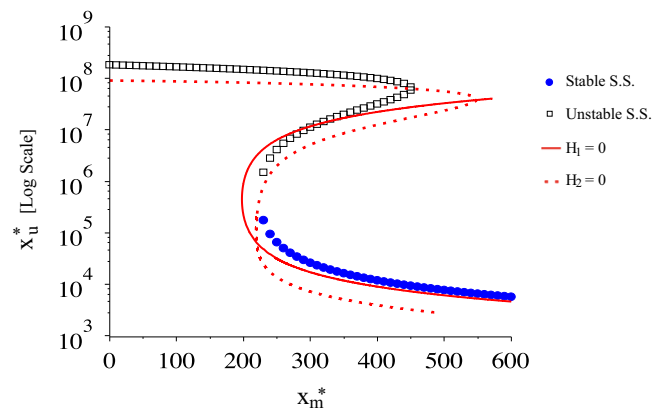


Fig. 2. Plots of the steady state tumour size x_u^* against the steady state memory size x_m^* . To show clearly what happens for small as well as large tumour sizes, we use a log scale for x_u^* . Stable steady states are indicated by blue circles and unstable states by black squares. We also plot the curves $H_1 = 0$ and $H_2 = 0$ in red (solid and dashed respectively), to indicate the boundaries which mark a change in stability. (For interpretation of the references to color in this figure caption, the reader is referred to the web version of this article.)

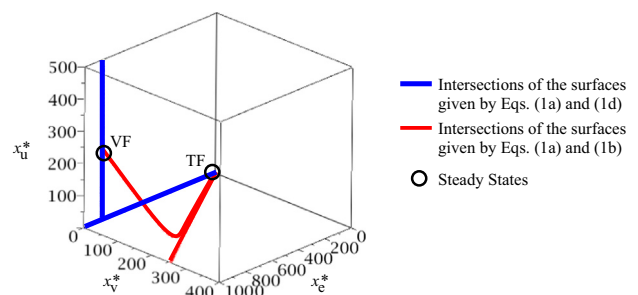


Fig. 3. A plot showing the intersections of surfaces described by Eqs. (1a), (1b) and (1d). Circled are the possible steady states for model (1), when $x_m = M$.

paper (also involved in the stability of these steady states) are summarised in Appendix A. Note that these values apply to tumour-immune interactions observed in mice.

Tumour-free steady states (TF): The tumour-free steady states are given by $(0, 0, x_m^*, 0, 0)$. These steady states are always unstable saddles, due to one positive eigenvalue $\lambda_1 = r > 0$. As such, this model predicts that the treatment protocol cannot lead to permanent tumour elimination. Thus, in the following, we will be concerned with investigating stable tumour-present steady states for which the tumour size is considered to be under control, i.e. below a certain threshold. For the purpose of this study, we will assume that the value of this threshold is 10^6 cells (which is the initial value for the number of cancer cells $x_u(0)$).

Tumour-present, virus-present, immune-free steady state (IF): The single immune-free steady state is given by $(x_u^*, x_i^*, 0, 0, x_v^*)$ where

$$x_u^* = \frac{\omega h_u}{bd_v - \omega}, \quad x_i^* = \frac{k - x_u^*}{1 + \frac{\delta k}{rx_u^*}} \quad \text{and} \quad x_v^* = \frac{\delta b}{\omega} \left(\frac{k - x_u^*}{1 + \frac{\delta k}{rx_u^*}} \right). \quad (2)$$

This steady state is identical to the immune-free steady state for the model introduced in Eftimie et al. (2011b). It can be easily shown (omitted here) that this state is always unstable and as such we do not consider it further.

Tumour-present, virus-free steady states (VF): For model (1), there are multiple virus-free steady states (in fact, infinitely many). We can gain insight into these steady states by plotting the surfaces described by the right-hand side of Eqs. (1a) and (1d) for x_m, x_e and x_u (since $x_v = x_i = 0$, it means that the remaining equations are satisfied trivially). In Fig. 1 we show the intersections of these two surfaces, corresponding to the virus-free steady states of the system. Two sets of steady states satisfy these intersection curves: the tumour-free (TF) steady states (i.e., $x_u = x_e = 0, x_m \in \mathbb{R}$, which have already been discussed above) and the tumour-present steady states (VF), which we focus on next. We observe that for the tumour-present states, the size of the tumour ranges from low (non-zero) values, which correspond to tumour being controlled by the immune system, to very large values (the carrying capacity size, k). To achieve a low steady state tumour-size there must be sufficiently high accompanying memory and effector cell populations.

Further insight can be gleaned by considering analytic solutions to Eqs. (1a) and (1d). In the following we denote the steady states of x_u, x_m and x_e by x_u^*, x_m^* and x_e^* , respectively. From Eq. (1d), we can obtain an expression for x_e^* in terms of x_u^* and x_m^* , which is given as

$$x_e^* = \frac{pe^{\lambda_m^*} h_v x_u^*}{d_e + d_t x_u^*}. \quad (3)$$

Substituting this expression into Eq. (1a) and considering only the tumour-present solutions yield the cubic equation

$$A(x_u^*)^3 + (B + Cx_m^*)(x_u^*)^2 + (D + Ex_m^*)x_u^* - F = 0, \quad (4)$$

where

$$A = rd_t h_e, \quad B = rh_e(d_e + d_t h_v - d_t k), \quad C = rp_e, \\ D = rh_e(d_e h_v - d_t h_v k - d_e k), \quad E = kp_e(d_u - r) \quad \text{and} \quad F = rkh_e d_e h_v. \quad (5)$$

Only real positive solutions of the cubic provide biologically relevant steady states. For any given x_m^* we may have between one and three steady states x_u^* .

To investigate the stability of these tumour-present virus-free steady states $(x_u^*, 0, x_m^*, x_e^*, 0)$, we observe that the five eigenvalues of the Jacobian calculated at the steady states are $\lambda = 0$ and the

two solutions of the quadratics

$$\lambda^2 + G_{1,2}\lambda + H_{1,2} = 0, \quad (6)$$

where

$$G_1 = \omega + \delta + d_u \frac{x_e^*}{h_e + x_e^*}, \quad (7a)$$

$$H_1 = \omega \left(\delta + d_u \frac{x_e^*}{h_e + x_e^*} \right) - \delta b d_v \frac{x_u^*}{h_u + x_u^*}, \quad (7b)$$

and

$$G_2 = \frac{2rx_u^*}{k} + d_u \frac{x_e^*}{h_e + x_e^*} - r + d_e + d_t x_u^*, \quad (8a)$$

$$H_2 = (d_e + d_t x_u^*) \left(\frac{2rx_u^*}{k} + d_u \frac{x_e^*}{h_e + x_e^*} - r \right) \\ + \frac{d_u h_e x_u^*}{(h_e + x_e^*)^2} \left(\frac{p_e h_v}{(h_v + x_u^*)^2} x_m^* - d_t x_e^* \right). \quad (8b)$$

Positive eigenvalues exist, and stability fails if either $H_1 < 0$ or $H_2 < 0$ (or both). In Fig. 2 we plot the states x_u^* against the states x_m^* given by the cubic (4), for the parameter values investigated in this paper (see Table A2). Here, we show also the threshold stability curves, $H_1 = 0$ and $H_2 = 0$. We note that only one branch of stable steady state solutions exists. Such states are characterised by a low (controlled) tumour size accompanied by a persistent memory cell population.

Tumour-present, virus-present, immune-present steady state (TVI): If all populations exist, the right-hand side of Eq. (1c) implies $x_m = M$. In Fig. 3 we plot the intersection curves of the surfaces given by the right-hand side of Eqs. (1a), (1b) and (1d), in terms of the steady state populations, x_u^*, x_v^* and x_e^* (using $x_m = M$ and replacing x_i with $\omega x_i^*/\delta b$, determined from the right-hand side of Eq. (1e)). We observe that there are only two distinct biologically relevant intersections of all three surfaces corresponding to steady states of model (1). Neither of these states, namely the TF steady state ($x_u = x_v = 0$) and a VF steady state ($x_u \approx 221, x_m = M = 10^4, x_e \approx 864$), has all five populations present. Thus, at least for the parameter values investigated in this paper (see Appendix A), a TVI state does not exist and as such we should concern ourselves with stabilising, at a low tumour size, the virus-free (VF) steady states discussed previously. Biologically, our concern with this VF state makes sense, as we would hope to find

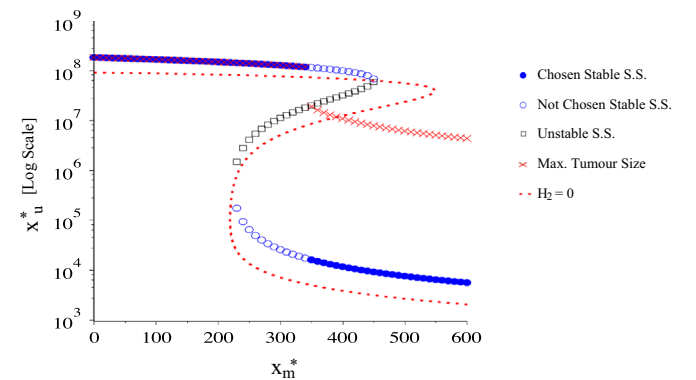


Fig. 4. Plot of the steady state tumour sizes x_u^* against the steady state memory sizes $x_m^* = x_m(0)$. To show more clearly what happens for small and large tumour sizes, we use a log scale for x_u^* . Stable steady states are indicated by blue circles and unstable by black squares. The dynamics of the system evolves towards the filled blue circles. We also include the curve $H_2 = 0$ (red dashed curve) to indicate the boundary which marks a change in stability and the maximum tumour size (red crosses) attained for each $x_m(0) = x_m^*$. (For interpretation of the references to color in this figure caption, the reader is referred to the web version of this article.)

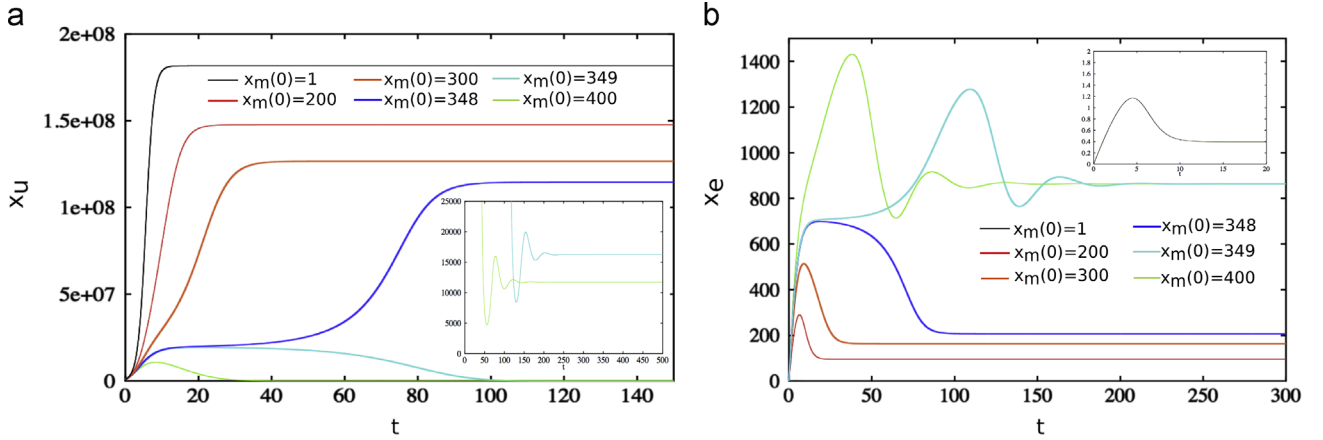


Fig. 5. Explicit time plots for (a) the uninfected tumour size and (b) the effector population for different values of the initial memory cell-population for virus-free initial conditions. In each case $x_u(0) = 10^6$ and $x_v(0) = x_i(0) = x_e(0) = 0$. All parameters are as in Table A2. Initial conditions are as in Table A1.

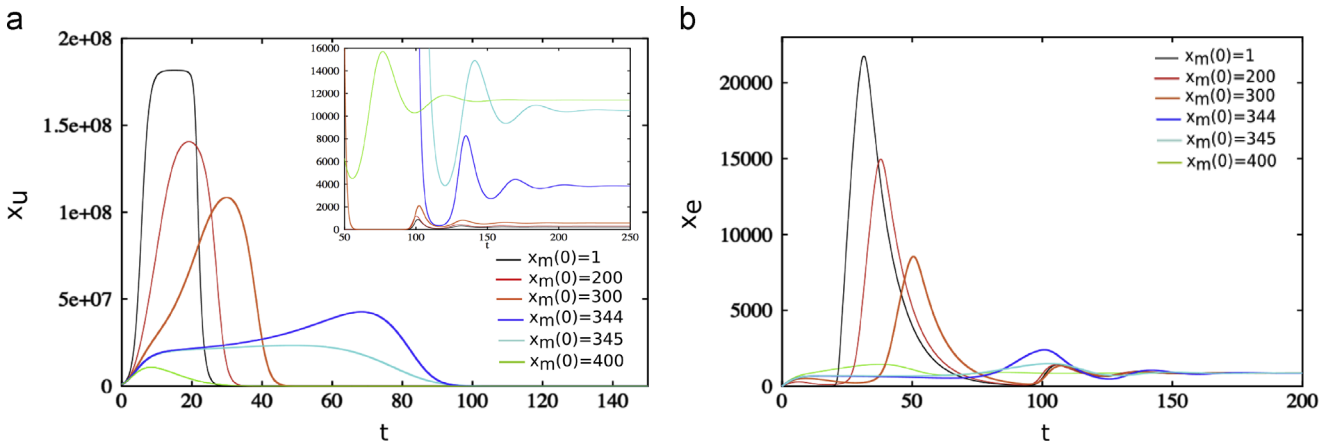


Fig. 6. Explicit time plots for (a) the uninfected tumour size, (b) the effector population for different values of the initial memory cell-population for virus-present initial conditions. In each case $x_u(0) = 10^6$, $x_v(0) = 1$ and $x_i(0) = x_e(0) = 0$. All parameters are as in Table A2. Initial conditions are as in Table A1.

a treatment protocol in which, after reducing the tumour size, the virus would be cleared.

4. A simplified virus-free system

Next, we consider a completely virus-free system. We will return to this model in the next sections, when we will investigate the role of the memory versus effector immune responses in tumour control. In the absence of the virus, system (1) reduces to

$$\frac{dx_u}{dt} = rx_u \left(1 - \frac{x_u}{k}\right) - d_u x_u \frac{x_e}{h_e + x_e}, \quad (9a)$$

$$\frac{dx_m}{dt} = 0, \quad (9b)$$

$$\frac{dx_e}{dt} = p_e \frac{x_u}{h_v + x_u} x_m - d_e x_e - d_t x_u x_e. \quad (9c)$$

The steady states (x_u^*, x_m^*, x_e^*) of this system still satisfy Eqs. (3) and (4). We note from Eq. (9b) that the memory cell population does not change and as such will remain at its initial size. Thus, we may consider $x_m^* = x_m(0)$. Therefore, the solutions for x_u^* obtained by solving (4) depend directly on the initial memory cell population size.

The eigenvalues of system (9a) are governed by

$$\lambda(\lambda^2 + G_2\lambda + H_2) = 0, \quad (10)$$

where G_2 and H_2 are given as before. Thus, stability of the

virus-free system is governed solely by the sign of H_2 . In Fig. 4 we plot the steady state tumour sizes, x_u^* , against the steady state memory size, x_m^* (as in Fig. 2, but now with only the $H_2 = 0$ stability boundary). We observe that for a range of x_m^* values ($x_m^* \approx 230 - 460$) the system is bistable. However, investigation of the long-term behaviour of system (9a) shows that the system always chooses one stable steady state (filled blue circles in Fig. 4(a)). We observe that the transition from the upper stable branch to the lower stable branch occurs as the maximum tumour size crosses the unstable branch (described by black squares). Hence, the unstable branch of steady states x_u^* acts as a separatrix: if the solution for x_u reaches any point above this branch the dynamics will approach the upper stable steady state; on the other hand, if the solution remains below this branch, the dynamics will approach the lower stable steady state. To indicate this, we also include the maximum tumour sizes attained for each $x_m(0) = x_m^*$ in Fig. 4 (see red crosses).

5. Tumour growth dynamics

In this section, we investigate the time-evolution of systems (1) and (9) towards the VF steady states described previously.

We start by discussing first the dynamics of the virus-free system (9a). In Fig. 5 we plot (a) the explicit time behaviour of the tumour population, and (b) the explicit time behaviour of the effector population, for different values of the initial memory cell

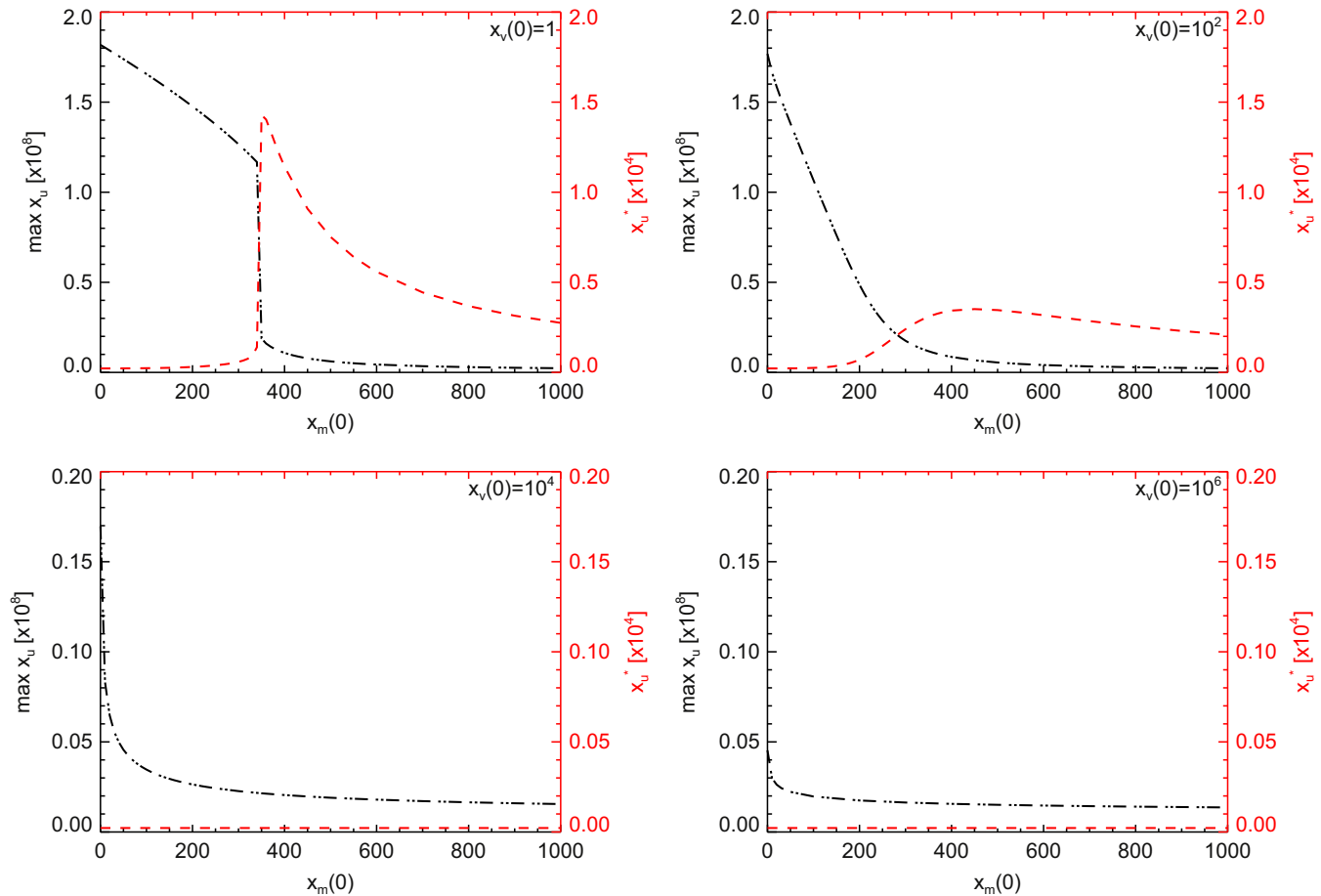


Fig. 7. Plots of the maximum tumour size (black dashed-dot curve) and the steady-state tumour size (red dashed curve), for different values of the initial virus population. The parameter values are as in Table A2. Initial conditions are as in Table A1. (For interpretation of the references to color in this figure caption, the reader is referred to the web version of this article.)

population $x_m(0)$. (The initial conditions for the other variables are $x_u(0) = 10^6$, $x_e(0) = x_v(0) = x_i(0) = 0$.) This plot corresponds directly with the behaviour predicted by Fig. 4: increasing the initial memory cell population leads to a lower steady state for the tumour size and a higher steady state for the effector population size. A substantial jump in tumour/effector size occurs between $x_m(0) = 348$ and $x_m(0) = 349$. When $x_m(0) = 348$ we observe a period of cancer dormancy (corresponding to a sustained “high” effector population size), between $t = 10$ and $t = 60$ days. However, the tumour begins to grow again and achieves a high steady-state size. When $x_m(0) = 349$ the system appears similarly dormant, but then tends to a much lower steady-state tumour size (low enough to be considered under control). When the steady state for the tumour population is on the lower branch of the stable solutions shown in Fig. 4, the effector population always tends towards the steady state $x_e^* \approx 864$ cells.

Note that the behaviour shown in Fig. 5 is for initial conditions with zero effector cells ($x_e(0) = 0$). If we add an initial effector cell population to the system, it has the effect of slightly reducing the value of $x_m(0)$ for which we achieve the jump to the lower steady-state branch for the tumour cells. For example, if $x_e(0) = 100$ we require $x_m(0) \geq 323$ to achieve the lower value of x_u^* .

We next consider the behaviour of the full system (1) (which is not virus-free, but evolves towards a virus-free steady state over time), as we vary the initial memory cell population. In Fig. 6 we plot (a) the explicit time behaviour of the tumour population, and (b) the explicit time behaviour of the effector population, for different values of the initial memory cell population $x_m(0)$. In Fig. 6(a) we observe that introducing a single virus particle

reduces the tumour size to a low and controlled steady state, for all values of $x_m(0)$. Fig. 2 predicted that only low tumour sizes for VF states were stable. Note that for low $x_m(0)$ values, the tumour first grows towards a very large “fatal” size, before decaying to a low steady-state value. Thus, as we vary $x_m(0)$, it becomes important to consider not only the steady state tumour size but also the maximum tumour size. Fig. 6(b) shows that in each case the effector population tends to $x_e^* \approx 864$.

Unexpected dynamics can be seen in the inset to Fig. 6(a): increasing $x_m(0)$ leads to an increase in the steady-state x_u^* . To get a better understanding of why this happens, in Fig. 7 we plot both the maximum tumour size and the steady-state tumour size against the initial memory population size $x_m(0)$, for $x_v(0) = \{1, 10^2, 10^4, 10^6\}$. As observed in Fig. 7(a), when we introduce one virus particle, a low initial memory population gives rise to a low steady-state tumour size. However, this behaviour is also accompanied by a higher peak in the tumour size. As we increase $x_m(0)$, the maximum tumour size decreases while the steady-state value for the tumour increases. This increasing/decreasing behaviour becomes particularly strong for $x_m(0) \in (340, 350)$. Note that for $x_m(0) > 430$, the maximum tumour sizes and the steady-state tumour sizes are below the thresholds of 10^7 and 10^6 cells, respectively. These thresholds are sufficiently low to ensure the survival of the mice. In Fig. 7(b) (where $x_v(0) = 10^2$), the sharp changes in both the maximum tumour size and the steady-state size are no longer observed. Instead both profiles are continuous and the steady-state size achieves a much lower peak. As we increase the initial virus population further (see Fig. 7(c)), the maximum tumour size reduces more rapidly, while the steady-state tumour size remains almost constant at $x_u^* \approx 221$ cells, far below the threshold of 10^6 cells.

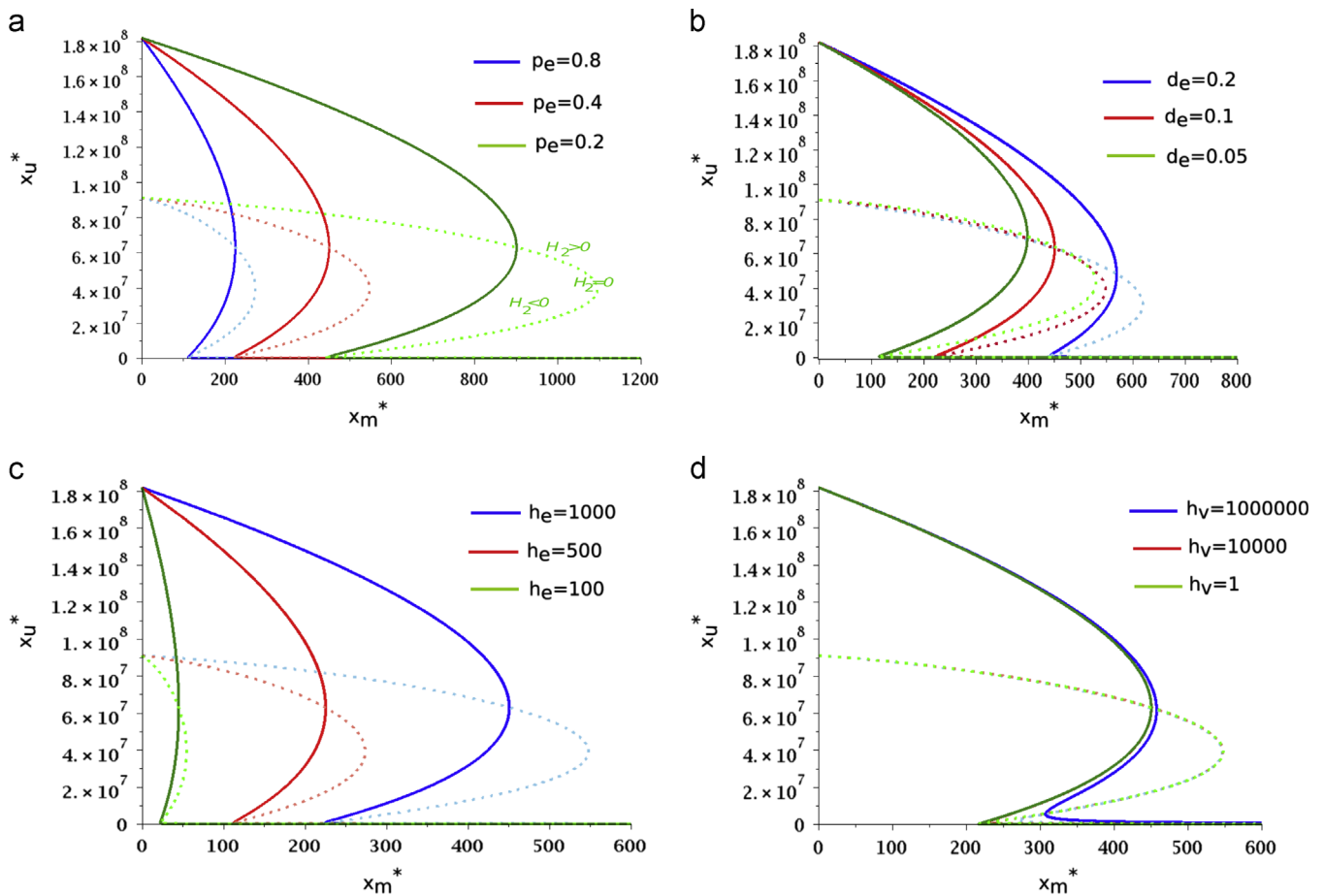


Fig. 8. Plots showing the steady state behaviour (solid curves) of the virus-free system along with stability boundaries $H_2 = 0$ (dashed curves) for different parameters. In panel (a) we change p_e , in panel (b) we change d_e , in panel (c) we change h_e and in panel (d) we change h_v , while keeping all other parameters fixed as in Table A2. Initial conditions are as in Table A1.

We do note, however, that even when $x_v(0) = 10^6$ and there is a high initial memory population size (see Fig. 7(d)), the peak of the tumour size is above 10^6 cells (although the attained size is short-lived and not typically fatal).

6. Memory versus immune responses on tumour growth

To compare the importance of the memory versus immune responses in tumour elimination, we focus on the simplified virus-free system. In Fig. 8, we graph the steady states x_u^* against the steady states x_m^* (equivalent to the initial memory population in this case) along with the stability boundary $H_2 = 0$, while changing different parameters that control the effector immune response. In Fig. 8(a) we change the rate p_e that controls the de-differentiation of memory cells into effector cells. Increasing this rate reduces the required initial memory size to achieve a lower steady-state tumour size.

Decreasing the natural effector decay rate d_e (see Fig. 8(b)) also leads to a reduction in the initial memory size required to achieve a lower steady-state tumour size. Similar results are obtained when decreasing the effector half-saturation constant h_e (see Fig. 8(c)). In Fig. 8(d) we include a plot which shows the effect of changing h_v . We see here that there are almost no differences in the long-term behaviour of system (1) when $1 < h_v < 10^4$. However, for $h_v = 10^6$ there are small differences in the size of x_u^* approached by system (1), for initial memory population sizes $x_m^* \in (200, 450)$.

We observed above (see Fig. 5 for the virus-free system and Fig. 6 for the virus-present system) that a low steady-state tumour size was accompanied by an effector steady-state size of $x_e^* \approx 864$ cells. To achieve this steady-state effector population size we must either have a high enough initial memory population or, as shown in Fig. 8, be able to control immune-related parameters i.e., provoke a higher de-differentiation of memory cells to effector cells, reduce the effector cell natural decay and enhance effector–tumour interactions. However, it might not be possible to control these parameters experimentally. And even if we can alter them favourably, a higher initial memory population size continues to be important. As such, we conclude that focus should remain on stimulating a high initial memory population.

7. Discussion

In this paper, we introduced a simple, nonlinear mathematical model that described the interactions among immune cells, cancer cells and viruses. Although the original purpose of the model was to investigate the dynamics of oncolytic therapy, much of what we have shown applies to a model of a virus-free system. As such, the model could be used to give insight into immune–cancer interactions after the stimulation of anti-cancer immune memory cells. We focussed our attention on the importance of memory and effector cell population sizes on stabilising the tumour-present virus-free steady states.

We found that for our model (system (1)) the dynamic behaviour always evolved towards a tumour-present virus-free

steady state, whether under virus-free or virus-present initial conditions. When the system was fully virus-free, we found that only by increasing the initial memory cell population could we achieve reduced tumour growth and low steady-state tumour size. For the virus-present system, it was important to have a high initial memory cell population in order to reduce the initial growth (and maximum size) of the tumour (although there was a slight trade-off as the steady-state size increased as we increased $x_m(0)$). Having a high initial memory cell population became less important as we increased the initial virus population, $x_v(0)$. Indeed when $x_v(0) = 10^6$ there was very little difference in the maximum tumour size and no difference in the steady-state tumour size, for all values of $x_m(0)$. A parameter investigation showed that provoking a high initial memory population would always lead to a positive outcome, and that biologically this is likely to be more attainable than stimulating changes to the immune-related parameters. Importantly, we have found that low steady-state tumour sizes were always accompanied by a high steady state effector population (always around $x_e^* \approx 864$ cells). As such, this adds to the evidence that suggests that cancer control is the result of a persisting population of effector cells, regardless of the initial number immune cells (Baitsch et al., 2011; Paulis et al., 2013; Berezhnoy et al., 2014).

Our investigations also indicated that specific conditions could lead to immune-mediated cancer dormancy. It is now evident from the literature that cancers may remain dormant for prolonged periods of time, after which tumours will either escape (and grow excessively) or be eliminated. Here, we showed that very slight changes to the system set-up (in our case slight changes to the initial memory cell population) could lead to a change between these two contrasting outcomes. Furthermore, with a wide range of parameters it is unlikely that we could predict whether the patient would go on to experience cancer growth or cancer reduction and control after dormancy. Unfortunately due to the very nature of cancer dormancy (i.e., cancer is at a very small size), it is often elusive to the methods of detection currently available to clinicians. Our findings remind us that it remains of great importance to search for ways to detect and monitor cancer dormancy.

Having discussed our results, we wish to stress that they are subject to the limitations of our model. As mentioned when we introduced the model set up, there are alternative ways of incorporating the biological mechanisms known to occur (e.g., exponential or Gompertzian tumour growth, bi-linear tumour-immune and tumour-virus interactions). Moreover, in this study we have only attempted to describe certain biological pathways that are still not fully understood. Different formulations of the model could well provide further insight into the role of effector and memory cells; in fact the subject may benefit from a detailed investigation of general interaction terms. However, our investigation into this important immunological problem aims to be a starting point for further discussion on this topic.

Acknowledgments

R.E. acknowledges support from an Engineering and Physical Sciences Research Council (UK) First Grant number EP/K033689/1.

Appendix A

Tables A1 and A2.

Table A1
Initial values of the variables for the model given by Eqs. (1a)–(1e).

Variables	Meaning	Initial value
x_u	Uninfected cancer cells	10^6
x_i	Infected cancer cells	0
x_m	Memory cells	$1 - 10^4$
x_e	Effector cells	0
x_v	Virus particles	$0 - 10^6$

Table A2

Model parameters and values used for numerical simulations. The majority of parameters are as in Eftimie et al. (2011b) (or at least within the ranges given). Throughout this report, we consider the density of cells (i.e., cell numbers per blood volume (vol)) and the plaque-forming units (PFU) for the virus particles. (PFU is a generally accepted functional measurement for the virus particles; defective viruses which do not form a plaque cannot infect their target and are discounted.)

Param.	Value	Units	Description and references
r	0.927	days ⁻¹	Proliferation rate for tumour cells (Bridle et al., 2010)
k	1.8182×10^8	cells/vol	Carrying capacity for the tumour cells (Bridle et al., 2010; N.I.H., O.A.C.U., 1996)
d_v	0.0038	(cells/vol)(PFU/vol) ⁻¹ (days) ⁻¹	Infection rate of tumour cells with the oncolytic virus
d_u	2.0	days ⁻¹	Lysis rate of tumour cells (infected and uninfected) by the immune cells (Kündig et al., 1996)
h_u	1	cells/vol	Half-saturation constant for the tumour cells infected with the oncolytic virus
h_e	10^3	cells/vol	Half-saturation constant for the effector cells that support half the maximum killing rate
h_v	10^4	PFU/vol	Half-saturation constant of (viral and tumour) antigens that induce half the maximum proliferation rate of immune cells
δ	1	days ⁻¹	Rate at which the oncolytic virus kills the tumor cells
p_m	2.5	days ⁻¹	Proliferation rate of memory cells following secondary encounter with tumor antigens carried by virus particles (Bridle et al., 2010)
M	10^4	(cells)/vol	Carrying capacity for memory cells
p_e	0.4	days ⁻¹	Rate at which memory cells become effector cells following secondary encounter with tumor antigens carried by virus particles
d_e	0.1	days ⁻¹	Death rate of effector cells (Bridle et al., 2010)
d_t	5×10^{-9}	(cells) ⁻¹ (vol)(days) ⁻¹	Inactivation rate of immune effector cells by the tumor cells
ω	2.042	days ⁻¹	Decay rate for the concentration of oncolytic virus (VSV) particles in the blood
b	1000	(PFU/vol)(cell) ⁻¹ (vol)	Number of virus (VSV) particles released from an infected cell, capable of forming plaques

References

- Almog, N., 2010. Molecular mechanisms underlying tumor dormancy. *Cancer Lett.* 294 (2), 139–146.
- Antia, R., Pilyugin, S., Ahmed, R., 1998. Models of immune memory: on the role of cross-reactive stimulation, competition, and homeostasis in maintaining immune memory. *Proc. Natl. Acad. Sci. U.S.A.* 95 (25), 14926–14931.
- Bachmann, M.F., Jennings, G.T., 2010. Vaccine delivery: a matter of size, geometry, kinetics and molecular patterns. *Nat. Rev. Immunol.* 10 (November (11)), 787–796.
- Baitsch, L., Baumgaertner, P., Devèvre, E., Raghav, S.K., Legat, A., Barba, L., Wiecekowsk, S., Bouzourene, H., Deplancke, B., Romero, P., Rufer, N., Speiser, D.E., 2011. Exhaustion of tumor-specific cd8 t cells in metastases from melanoma patients. *J. Clin. Invest.* 121 (June (6)), 2350–2360.
- Bajzer, Z., Carr, T., Josić, K., Russell, S., Dingli, D., 2008. Modeling of cancer virotherapy with recombinant measles viruses. *J. Theor. Biol.* 252, 109–122.
- Benzekry, S., Lamont, C., Beheshti, A., Tracz, A., Ebos, J.M.L., Hlatky, L., Hahnfeldt, P., 2014. Classical mathematical models for description and prediction of experimental tumor growth. *PLoS Comput. Biol.* 10 (August (8)), e1003800.
- Berezchnoy, A., Rajagopalan, A., Gilboa, E., 2014. A clinically useful approach to enhance immunological memory and antitumor immunity. *Oncolimmunology* 3, e28811.
- Biesecker, M., Kimn, J.-H., Lu, H., Dingli, D., Bajzer, Z., 2010. Optimization of virotherapy for cancer. *Bull. Math. Biol.* 72 (2), 469–489.
- Bonate, P., 2011. Modeling tumour growth in oncology. In: Bonate, P., Howard, D. (Eds.), *Pharmacokinetics in Drug Development. Advances and Applications* vol. 3. Springer, US.
- Bozic, I., Allen, B., Nowak, M.A., 2012. Dynamics of targeted cancer therapy. *Trends Mol. Med.* 18, 311–316.
- Breitbach, C., Paterson, J., Lemay, C., Falls, T., McGuire, A., Parato, K., Stojdl, D., Daneshmand, M., Speth, K., Kirn, D., McCart, J., Atkins, H., Bell, J., 2007. Targeted inflammation during oncolytic virus therapy severely compromises tumor blood flow. *Mol. Therapy* 15 (9), 1686–1693.
- Bridle, B., Stephenson, K., Boudreau, J., Koshy, S., Kazhdan, N., Pullenayegum, E., Brunellière, J., Bramson, J., Lichty, B., Wan, Y., 2010. Potentiating cancer immunotherapy using an oncolytic virus. *Mol. Therapy* 18, 1430–1439.
- Crotty, S., Ahmed, R., 2004. Immunological memory in humans. *Semin. Immunol.* 16, 197–203.
- Dermime, S., Armstrong, A., Hawkins, R., Stern, P., 2002. Cancer vaccines and immunotherapy. *Br. Med. Bull.* 62, 149–162.
- Eftimie, R., Bramson, J.L., Earn, D.J.D., 2011a. Interactions between the immune system and cancer: a brief review of non-spatial mathematical models. *Bull. Math. Biol.* 73 (1), 2–32.
- Eftimie, R., Dushoff, J., Bridle, B., Bramson, J., Earn, D., 2011b. Multi-stability and multi-instability phenomena in a mathematical model of tumor-immune-virus interactions. *Bull. Math. Biol.* 73 (12), 2932–2961.
- Farrar, J., Katz, K., Windsor, J., Thrush, G., Scheuermann, R., Uhr, J., Street, N., 1999. Cancer dormancy. VII. A regulatory role for CD8⁺ T cells and IFN- γ in establishing and maintaining the tumour-dormant state. *J. Immunol.* 162, 2842–2849.
- Ferreira Jr., S.C., Martins, M.L., Vilela, M.J., 2005. Fighting cancer with viruses. *Physica A* 345, 591–602.
- Friedman, A., Tian, J., Fulci, G., Chiocca, E., Wang, J., 2006. Glioma virotherapy: effects of innate immune suppression and increased viral replication capacity. *Cancer Res.* 66 (4), 2314–2319.
- Gajewski, T., Schreiber, H., Fu, Y.-X., 2013. Innate and adaptive immune cells in the tumor microenvironment. *Nat. Immunol.* 14 (10), 1014–1022.
- Gatenby, R., 2009. A change of strategy in the war on cancer. *Nature* 459, 509.
- Guiot, C., Degiorgis, P., Delsanto, P., Gabriele, P., Diesboeck, T., 2003. Does tumour growth follow a “universal law”? *J. Theor. Biol.* 225, 147–151.
- Ikeda, K., Ichikawa, T., Wakimoto, H., Silver, J., Deisboeck, T., Finkelstein, D., Harsh IV, G., Louis, D., Bartus, R., Hochberg, F., Chiocca, E., 1999. Oncolytic virus therapy of multiple tumors in the brain requires suppression of innate and elicited antiviral responses. *Nat. Med.* 5 (8), 881–887.
- Kaech, S., Wherry, J., Ahmed, R., 2002. Effector and memory t-cell differentiation: implications for vaccine development. *Nat. Rev. Immunol.* 2, 251–262.
- Karev, G.P., Novozhilov, A.S., Koonin, E.V., 2006. Mathematical modeling of tumor therapy with oncolytic viruses: effects of parametric heterogeneity on cell dynamics. *Biol. Direct.* 1, 30.
- Kelly, E., Russell, S.J., 2007. History of oncolytic viruses: genesis to genetic engineering. *Mol. Therapy* 15, 651–659.
- Klebanoff, C.A., Gattinoni, L., Restifo, N.P., 2006. CD8⁺ T-cell memory in tumor immunology and immunotherapy. *Immunol. Rev.* 211, 214–224.
- Klebanoff, C.A., Gattinoni, L., Torabi-Parizi, P., Kerstann, K., Cardones, A.R., Finkelstein, S.E., Palmer, D.C., Antony, P.A., Hwang, S.T., Rosenberg, S.A., Waldmann, T.A., Restifo, N.P., 2005. Central memory self tumor-reactive CD8⁺ T cells confer superior antitumor immunity compared with effector memory T cells. *Proc. Natl. Acad. Sci.* 102, 9571–9576.
- Komarova, N.L., Wodarz, D., 2010. Ode models for oncolytic virus dynamics. *J. Theor. Biol.* 263 (4), 530–543.
- Kumar, H., Kawai, T., Akira, S., 2011. Pathogen recognition by the innate immune system. *Int. Rev. Immunol.* 30 (1), 16–34.
- Kündig, T., Bachmann, M., Oehen, S., Hoffmann, U., Simard, J., Kalberer, C., Pircher, H., Ohashi, P., Hengartner, H., Zinkernagel, R., 1996. On the role of antigen maintaining cytotoxic T-cell memory. *Proc. Natl. Acad. Sci. U.S.A.* 93, 9716–9723.
- Laird, A., 1964. Dynamics of tumor growth. *Br. J. Cancer* 18, 490–502.
- Looney, W., Ritenour, E., Hopkins, H., 1980. Changes in growth rate of an experimental solid tumour following increasing doses of cyclophosphamide. *Cancer Res.* 40, 2179–2183.
- Marusić, M., Vuk-Pavlovic, S., 1993. Prediction power of mathematical models for tumour growth. *J. Biol. Syst.* 1 (1), 69–78.
- N.I.H., O.A.C.U., 1996. Guidelines for Endpoints in Animal Study Proposals. (http://oacu.od.nih.gov/ARAC/documents/ASP_Endpoints.pdf).
- Paiva, L.R., Binny, C., Ferreira Jr., S.C., Martins, M.L., 2009. A multiscale mathematical model for oncolytic virotherapy. *Cancer Res.* 69 (February (3)), 1205–1211.
- Paiva, L.R., Martins, M.L., Ferreira Jr., S.C., 2011. Questing for an optimal, universal viral agent for oncolytic virotherapy. *Phys. Rev. E* 84, 041918.
- Paulis, L., Mandal, S., Kreutz, M., Figdor, C., 2013. Dendritic cell-based nanovaccines for cancer immunotherapy. *Curr. Opin. Immunol.* 25, 389–395.
- Pol, J.G., Ressaëguier, J., Lichty, B.D., 2012. Oncolytic viruses: a step into cancer immunotherapy. *Virus Adapt. Treat.* 4, 1–21.
- Quesnel, B., 2008. Dormant tumor cells as therapeutic target? *Cancer Lett.* 267, 10–17.
- Rommelfanger, D.M., Offord, C.P., Dev, J., Bajzer, Z., Vile, R.G., Dingli, D., 2012. Dynamics of melanoma tumor therapy with vesicular stomatitis virus: explaining the variability in outcomes using mathematical modeling. *Gene. Therapy* 19 (5), 543–549.
- Russell, S.J., Peng, K.-W., Bell, J.C., 2012. Oncolytic virotherapy. *Nat. Biotechnol.* 30 (7), 658–670.
- Sallusto, F., Geginat, J., Lanzavecchia, A., 2004. Central memory and effector memory t cell subsets: function, generation, and maintenance. *Annu. Rev. Immunol.* 22, 745–763.
- Teng, M., Swann, J., Koebel, C., Schreiber, R., Smyth, M., 2008. Immune-mediated dormancy: an equilibrium with cancer. *J. Leukoc. Biol.* 84, 988–993.
- Uhr, J., Pantel, K., 2011. Controversies in clinical cancer dormancy. *Proc. Natl. Acad. Sci. U.S.A.* 108, 12396–12400.
- van Duiker, S., Fransen, M.F., Redeker, A., Wiele, B., Platenburg, G., Krebber, W.-J., Ossendorp, F., Melief, C.J.M., Arens, R., 2012. Vaccine-induced effector-memory cd8⁺ t cell responses predict therapeutic efficacy against tumors. *J. Immunol.* 189 (7), 3397–3403.
- Wein, L.M., Wu, J.T., Kirn, D., 2003. Validation and analysis of a mathematical model of a replication-competent oncolytic virus for cancer treatment: implications for virus design and delivery. *Cancer Res.* 63, 1317–1324.
- Wherry, J.E., Ahmed, R., 2004. Memory cd8 t-cell differentiation during viral infection. *J. Virol.* 78 (11), 5535–5545.
- Wilkie, K., Hahnfeldt, P., 2013a. Mathematical models of immune-induced cancer dormancy and the emergence of immune evasion. *Interface Focus* 3, 20130010.
- Wilkie, K., Hahnfeldt, P., 2013b. Tumor-immune dynamics regulated in the micro-environment inform the transient nature of immune-induced tumor dormancy. *Cancer Res.* 3, 3534–3544.
- Wodarz, D., 2001. Viruses as antitumor weapons: defining conditions for tumor remission. *Cancer Res.* 61, 3501–3507.
- Wodarz, D., 2006. *Killer Cell Dynamics: Mathematical and Computational Approaches to Immunology*. Springer New York, USA.
- Wodarz, D., Hofacre, A., Lau, J.W., Sun, Z., Fan, H., Komarova, N.L., 2012. Complex spatial dynamics of oncolytic viruses in vitro: mathematical and experimental approaches. *PLoS Comput. Biol.* 8 (6), e1002547.
- Wodarz, D., Komarova, N., 2009. Towards predictive computational models of oncolytic virus therapy: basis for experimental validation and model selection. *PLoS One* 4 (1), e4271.
- Wu, J., Kirn, D., Wein, L., 2004. Analysis of a three-way race between tumor growth, a replication-competent virus and an immune response. *Bull. Math. Biol.* 66 (4), 605–625.
- Zhang, P., Côté, A.L., de Vries, V.C., Usherwood, E.J., Turk, M.J., 2007. Induction of post-surgical tumor immunity and t-cell memory by a poorly immunogenic tumor. *Cancer Res.* 67, 6468–6477.